

ESI

Supramolecular Nanotube Constructed from 3d-4f Heterometallic Sandwiched Polyoxotungstate Dimers

Han Xue,^a Zhong Zhang,^a Rui Pan,^a Bai-Feng Yang,^a Hong-Sheng Liu,^{*c} and Guo-Yu Yang ^{*ab}

^a*MOE Key Laboratory of Cluster Science, School of Chemistry, Beijing Institute of Technology, Beijing 100081, China*

^b*Department of Chemistry, Key Laboratory for Preparation and Application of Ordered Structural Materials of Guangdong Province, Shantou University, Shantou, Guangdong 515063, China*

^c*College of Chemical Engineering, Daqing Normal University; Key Laboratory of Oilfield Applied chemistry, College of Heilongjiang Province, Daqing, Heilongjiang 163712, China.*

Table S1. Bond Valence Sum (BVS) Calculations of All W, Fe and Ln Atoms in **1-4**.

Table S2. Variation of Ln–O Bond Lengths with the atomic number in **1-4**.

Figure S1 Comparison of the simulated and experimental PXRD patterns of **1-4**.

Figure S2 The IR spectrum of **1-4**.

Figure S3 UV-Vis plots of Kunelka-Munk function versus energy E (eV) of **1a**, **2b**, **3c**, **4d**.

Figure S4 The TG curve of **1-4**.

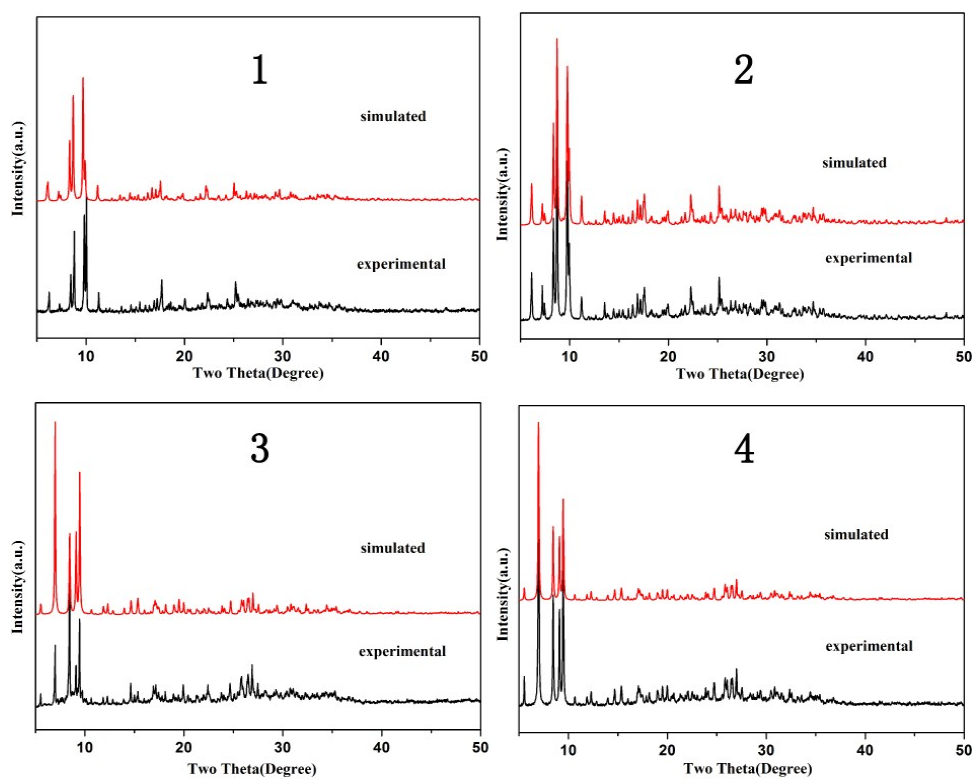
Figure S5 Coloration change of compound **1-3** after 0-330 min of UV irradiation with a 300 W xenon lamp.

Table S1. Bond Valence Sum (BVS) Calculations of All W, Fe and Ln Atoms in **1–4**.

1-BVS				2-BVS				3-BVS		4-BVS	
Ln1	3.24	W10	5.29	Ln1	2.95	W10	6.46	Ln1	3.26	Ln1	2.98
Fe1	3.08	W11	6.35	Fe1	3.14	W11	6.14	Fe1	3.23	Fe1	3.06
Fe2	3.11	W12	6.31	Fe2	3.13	W12	6.28	W1	6.03	W1	6.02
W1	6.09	W13	6.44	W1	5.93	W13	6.22	W2	5.95	W2	6.18
W2	5.81	W14	6.15	W2	6.33	W14	6.17	W3	6.40	W3	6.36
W3	5.99	W15	6.11	W3	6.28	W15	5.97	W4	6.10	W4	6.11
W4	5.80	W16	5.93	W4	6.14	W16	5.93	W5	5.91	W5	6.15
W5	6.34	W17	6.47	W5	6.06	W17	5.93	W6	6.09	W6	5.61
W6	5.62	W18	5.06	W6	6.05	W18	5.90	W7	5.65	W7	5.85
W7	6.47	W19	6.07	W7	6.13	W19	6.21	W8	5.66	W8	6.14
W8	5.33	W20	5.94	W8	6.19	W20	6.18	W9	5.95	W9	5.91
W9	5.94			W9	6.20			W10	5.89	W10	5.85

Table S2. Variation of Ln–O Bond Lengths with the atomic number in **1–4**.

Compounds _{atomic number}	Range of Ln–O Lengths (Å)	Average Ln–O lengths (Å)
1(La ^{III}) ₅₇	2.47(2)-2.589(18)	2.526
2(Ce ^{III}) ₅₈	2.458(15)-2.529(14)	2.515
3(Sm ^{III}) ₆₂	2.383(13)-2.471(15)	2.436
4(Tb ^{III}) ₆₅	2.378(15)-2.429(16)	2.397

**Figure S1** Comparison of the simulated and experimental PXRD patterns of **1–4**.

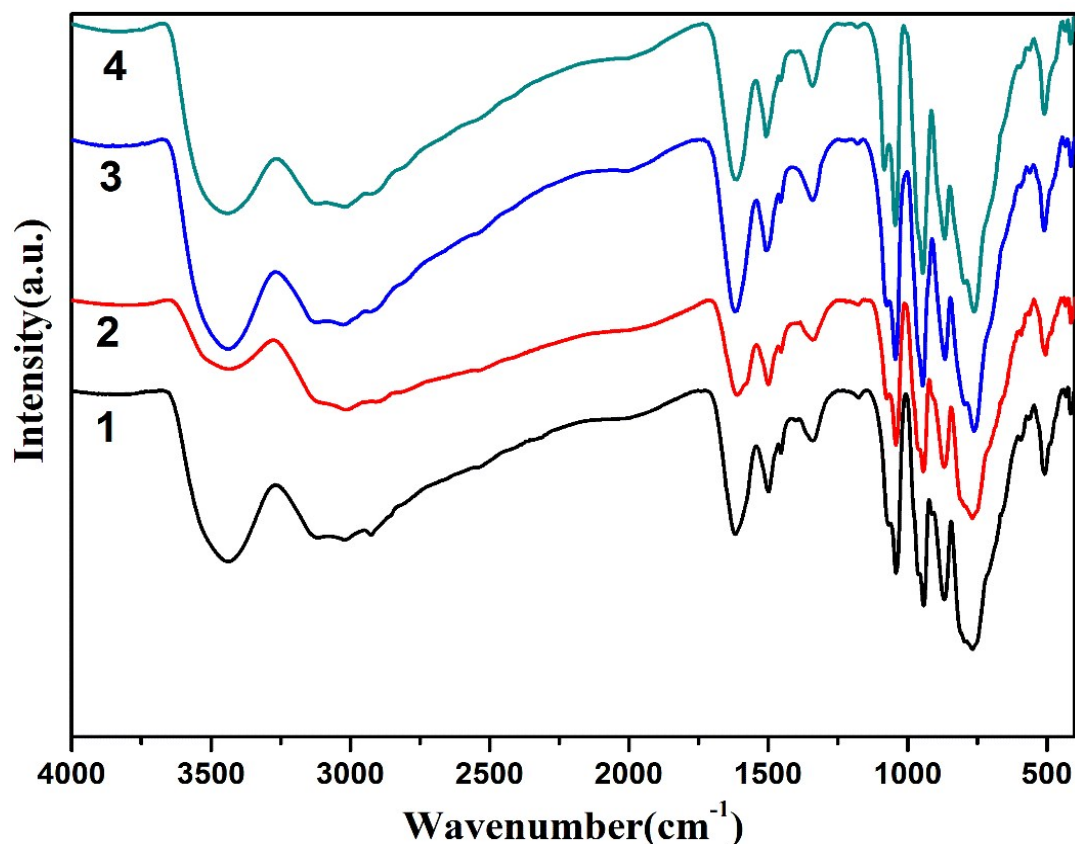


Figure S2 The IR spectrum of 1-4.

IR spectra.

The IR spectra of **1–4** were recorded with KBr pellets in the range of 4000–400 cm^{-1} (Figure S2). In the low wavenumber region, IR spectra of **1–4** all exhibit the characteristic $\nu_{\text{as}}(\text{P–O})$, terminal $\nu_{\text{as}}(\text{W–O}_{\text{t}})$, corner-sharing $\nu_{\text{as}}(\text{W–O}_{\text{b}})$ and edge-sharing $\nu_{\text{as}}(\text{W–O}_{\text{c}})$ asymmetric vibration patterns resulting from the Keggin-type POM framework, which are observed at 1066, 1041; 960, 942; 912, 867 and 794, 766 cm^{-1} for **1**, 1074, 1042; 963, 943; 868; 795, 767 for **2**, 1073, 1043; 945; 866; 794, 760 for **3**, 1083, 1044; 944; 867; 796, 760 for **4**, respectively. By a close examination of their IR spectra, some stretching vibration bands split into two bands as a consequence of the lower symmetry of the divacant poly-oxoanion fragments in **1–4** than those of the plenary Keggin POT clusters.¹ In contrast, IR spectra of **1–4** obviously differ from those of the trivacant Keggin polyoxoanion precursors,^{1,2} which further confirm the structural transformations from $[\alpha\text{-PW}_9\text{O}_{34}]^{9-}$ to $[\alpha\text{-PW}_{10}\text{O}_{38}]^{9-}$ during the course of forming **1–4**. Moreover, the resonances appearing at 3436; 3437; 3436; 3437 cm^{-1} and 3027; 3015; 3027; 3015 cm^{-1} are attributable to the $\nu(-\text{NH}_2)$ and $\nu(-\text{CH}_2)$ stretching vibration while the signals at 1617; 1611; 1619; 1613 cm^{-1} and 1454; 1454; 1455; 1455 cm^{-1} are assigned to the $\delta(-\text{NH}_2)$ and $\delta(-\text{CH}_2)$ bending vibration, respectively. For **1–4**, the resonances at 1498, 1340; 1499, 1341; 1507, 1341; 1506, 1341 cm^{-1} are attributed to the $\nu_{\text{as}}(\text{C=O})$ and $\nu_{\text{as}}(\text{C–O})$ stretching vibrations of acetate ligands, respectively.³ The occurrence of these characteristic signals confirms the presence of en groups and Tart ligands in **1–4**. In addition, the vibration bands at 3436–3437 cm^{-1} are indicative of the presence of lattice water molecules or coordination water molecules. In a word, the results of the IR spectra are in good agreement with those obtained from the X-ray single-crystal structural analyses.

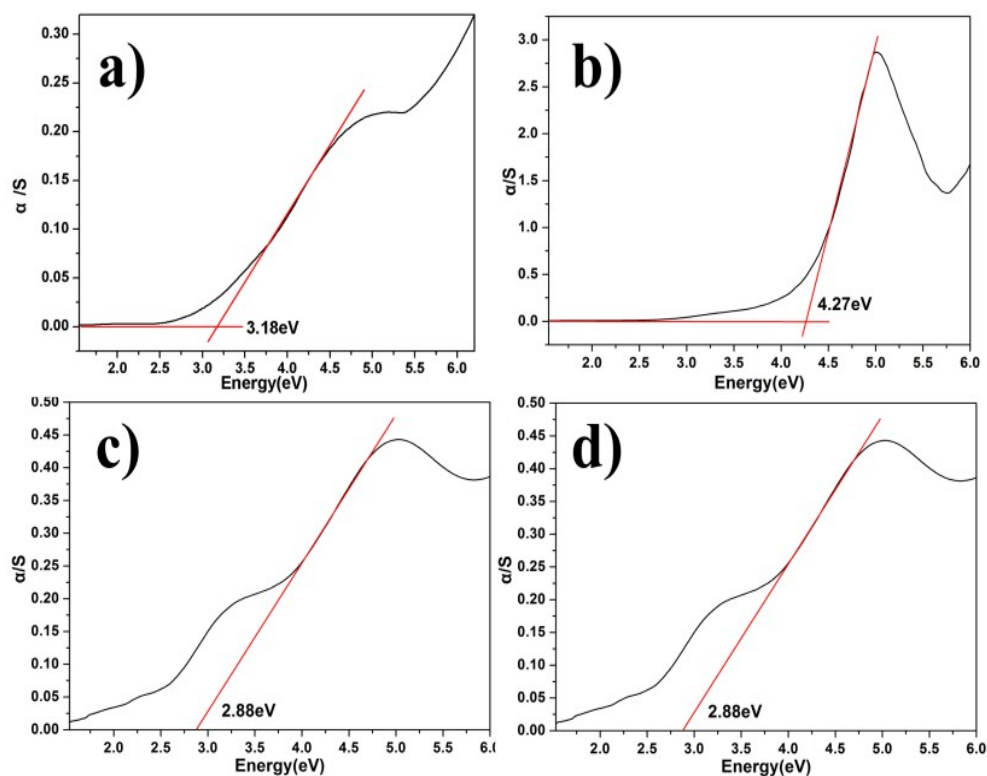


Figure S3 UV-Vis plots of Kubelka-Munk function versus energy E (eV) of **1** (a), **2** (b), **3** (c), **4** (d).

UV spectra

To evaluate the optical properties of **1-4**, the measurements of diffuse reflectance spectra for powdered crystal samples were performed to obtain their band gaps (E_g) (Figure S3). The band gap was determined as the intersection point between the energy axis and the line extrapolated from the linear portion of the absorption edge in a plot of the Kubelka–Munk function against the energy E .^{4,5} Their band gaps E_g are 3.18, 4.27, 2.88 and 2.88 eV for **1-4**, respectively. These band gaps are related to the energy-level difference between the oxygen p-type HOMO and the tungsten p-type LUMO.⁶ Similar behaviors have been observed in several reported TMSPs, such as $[\{Ni_6(\mu_3-OH)_3(en)_2(H_2O)_8\}(PW_9O_{34})]$ (en = ethylenediamine),⁷ $[Ni_6(enMe)_3(\mu_3-OH)_3]_3(Ac)_2(H_2O)(P_2W_{15}O_{56})_2]$ ($enMe$ = 1,2-diaminopropane).⁸ The band gaps of the compounds decrease with increasing dimensionality or complexity of the structures, as pointed out by Kanatzidis and Papavassiliou.⁹⁻¹¹

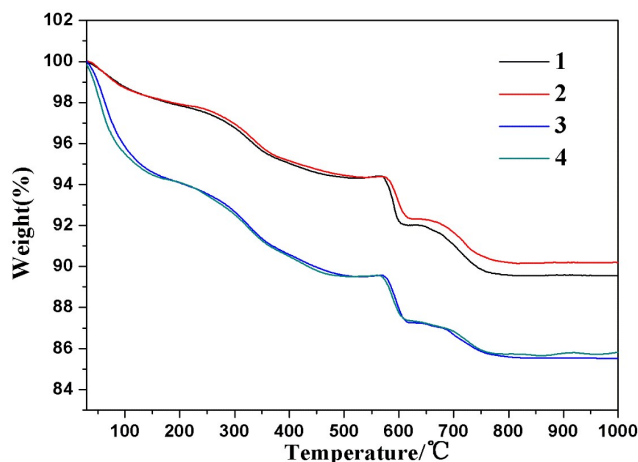


Figure S4 The TG curve of **1-4**.

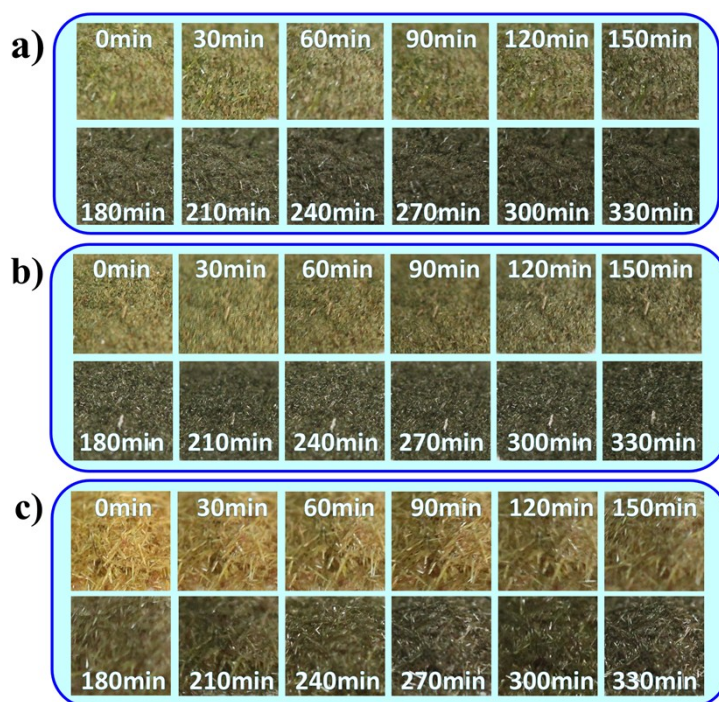


Figure S5 Coloration change of compound 1-3 after 0-330 min of UV irradiation with a 300 W xenon lamp,

1 (a), 2 (b), 3 (c).

References:

- 1 A. P. Ginsberg, *Inorganic Syntheses*. New York: John Wiley. Sons 1990, **27**, 100.
- 2 J. W. Zhao, J. Luo, L. J. Chen, J. Yuan, H. Y. Li, P. T. Ma, J. P. Wang and J. Y. Niu, *CrystEngComm*, 2012, **14**, 7981.
- 3 J. Y. Niu, K. H. Wang, H. N. Chen, J. W. Zhao, P. T. Ma, J. P. Wang, M. X. Li, Y. Bai and D. B. Dang, *Cryst. Growth Des.*, 2009, **9**, 4362.
- 4 W. M. Wesley and W. G. H. Harry, *Reflectance Spectroscopy*, Wiley (New York, 1966).
- 5 J. I. Pankove, *Optical Processes in Semiconductors*, Prentice-Hall (New York, 1997).
- 6 Y. Xia, P. Wu, Y. Wei, Y. Wang and H. Guo, *Cryst. Grow. Des.*, 2006, **6**, 253.
- 7 J. W. Zhao, H. P. Jia, J. Zhang, S. T. Zheng and G. Y. Yang, *Chem. -Eur. J.* 2007, **13**, 10030.
- 8 X. X. Li, W. H. Fang, J. W. Zhao and G. Y. Yang, *Chem. Eur. J.* 2014, **20**, 17324.
- 9 E. A. Axtell, Y. Park, K. Chondroudis and M. G. Kanatzidis, *J. Am. Chem. Soc.*, 1998, **120**, 124.
- 10 G. C. Papavassiliou, *Prog Solid. State. Chem.* 1997, **25**, 125.
- 11 T. Yamase, *Chem. Rev.*, 1998, **98**, 307.